(32) Leyte, J. C.; Zuiderweg, L. H.; Vledder, H. J. *Spectrochim. Acta* **1967**, *23A*, 1397.
(33) Lippincott, E. R.; Schroeder, R. *J. Chem. Phys.* **1955**, *23*, 1099.
(34) Poland, D.; Scheraga, H. A. *Biochemistry* **1967**, *6*, 3791.
(35) Hopfinger, A. J. *Conformational Properties of Macromolecules*; Academic Press: New York, 1973.
(36) Ninomiya, A.; Toei, K. *Nippon Kagaku Zasshi* **1969**, *90*, 655.
(37) Manning, G. S. *J. Chem. Phys.* **1969**, *51*, 924.

Diffusion of Weakly Confined Star and Linear Polymers and Strongly Confined Linear Polymers in a Porous Material

Nalini Easwar† and Kenneth H. Langley*

Department of Physics and Astronomy, University of Massachusetts, Amherst, Massachusetts 01003

F. E. Karasz

Polymer Science and Engineering Department, University of Massachusetts, Amherst, Massachusetts 01003. *Received January 19, 1989; Revised Manuscript Received May 23, 1989*

ABSTRACT: We report the direct measurement, by dynamic light scattering, of the macroscopic diffusion coefficient D_∞ (at low q) of linear, four-arm star and eight-arm star polyisoprene in silica controlled pore glass, for values of the confinement parameter $\lambda_H = R_H/R_p < 0.1$, where R_H is the hydrodynamic radius of the polymer and R_p is the radius of the pores in the glass. The reduced diffusion in the pores is found to depend on the molecular architecture of the polymer. For a given λ_H, the branched polymers diffuse slower than the linear polymer; it is also found that eight-arm stars diffuse more slowly than four-arm stars of the same hydrodynamic radius. The results are compared to hydrodynamic theories for hard spheres in isolated cylindrical pores. Our results indicate that the hydrodynamic radius of a polymer derived from its diffusion coefficient in dilute unbounded solution does not uniquely describe the hydrodynamic effects of a constraining wall on its diffusion behavior. We also report measurements of the macroscopic diffusion D_∞ of strongly confined linear polystyrene chains with λ_H values up to 0.74. Over the range of confinement investigated, an asymptotic region described by a power law relationship between D_∞ and molecular weight is not observed. Our data suggest that the presence of two length scales in the porous material could play an important role in the diffusion of strongly confined chains, in accordance with the theoretical model of Muthukumar and Baumgartner.

Introduction

The study of polymer transport in porous media has theoretical importance as well as relevance to many phenomena of technological and scientific interest. Experiments such as transport across track-etched membranes,[1-4] transcient diffusion into porous glass,[5,6] and broadening of chromatographic peaks[7] have been directed toward relating macroscopic diffusion to the microscopic parameters characterizing the polymer and the porous medium. The major disadvantage of these phenomenological techniques is that knowledge of the boundary layer resistance to transport and the equilbrium partitioning coefficient of the polymer between the unbounded solution and the pore space are necessary for the interpretation of the data. Attempts to explore directly the movement of molecules *within* the porous medium have employed the experimental techniques of forced Rayleigh scattering,[8] pulsed field-gradient spin-echo NMR,[9] and quasi-elastic light scattering.

Recently, Bishop et al.[10,11] have reported the direct measurement of the diffusion of linear flexible polystyrene in porous glasses by quasi-elastic light scattering (QELS). This technique has the advantage of probing directly the diffusion in pores inside a single fragment of porous material, under thermodynamic equilibrium conditions. These measurements showed that the reduced diffusion in the controlled pore glasses relative to the unbounded solution can be understood in terms of structural effects and hydrodynamic interactions, which are separable phenomena. For small λ_H, the diffusion of these polymers can be considered as the diffusion of equivalent hard spheres. Data for $0 < \lambda_H < 0.23$ fit well to the Brenner and Gaydos theory[12] for the diffusion of hard spheres in isolated cylindrical pores. The plots also yielded values for the intrinsic conductivity X_0 of these glasses. As the ratio of the size of the polymer to that of the pore increased, the hydrodynamics of the confined flexible polymers showed a transition from non-free draining (analogous to hard sphere) to free draining (analogous to Rouse chain) behavior. The maximum confinement parameter reached in these measurements was $\lambda_H = 0.47$.

The research reported in this paper extends the previous work by addressing two aspects of polymer diffusion, namely, the effects of molecular architecture and that of strong confinement on the reduced diffusion in the pores. First, the effect of molecular architecture has been investigated by comparing, in three different porous glasses, the diffusion of star polymers of different arm number but comparable molecular weight. A compari-

† Present Address: Department of Physics, Smith College, Northampton, MA 01063.

0024-9297/90/2223-0738$02.50/0

Table I
Characteristics of Linear and Star Polymer Samples

polymer	code	mol wt[a]	$\bar{M}_w/M_n$	source
		$10^{-3}\bar{M}_w$		
four-arm polyisoprene	PI4-47	46.5	<1.1	University of Akron, Akron, OH
eight-arm polyisoprene	PI8-41	41.0	<1.1	University of Akron, Akron, OH
		$10^{-3}\bar{M}_p$		
linear polyisoprene	PI-60A	60.46	1.04	PolySciences, Inc.
	PI-60B	60.00	1.04	Polymer Laboratories Ltd.
	PI-34	34.00	1.04	Polymer Laboratories Ltd.
linear polystyrene	PS-1030	1030	1.06	Polymer Laboratories Ltd.
	PS-1400	1400	1.05	Polymer Laboratories Ltd.
	PS-2050	2050	1.06	Polymer Laboratories Ltd.
	PS-2950	2950	1.06	Polymer Laboratories Ltd.
	PS-4400	4400	1.06	Polymer Laboratories Ltd.

[a] M_p = peak molecular weight from size-exclusion chromatography.

son of the diffusion of stars with that of linear chains of comparable molecular weight has also been made. These measurements attempt to answer the question of whether the hydrodynamic radius of a flexible polymer is the proper length scale to use in describing the hydrodynamic polymer–wall interactions. A comparative study such as ours of the restricted diffusion of star and linear polymers has been done recently in porous membranes.[13] In the membrane study, star-branched polymers were found to diffuse more slowly through the pores than linear chains of the same hydrodynamic radius, in qualitative agreement with recent results on size exclusion chromatography of branched polymers[14,15] and with our results. However, the results of the membrane study did not agree with a theoretical model that combines the pore partitioning coefficient of random flight chains with the hydrodynamic resistance of hard spheres. The second aspect of polymer diffusion addressed in this paper is the movement of strongly confined linear chains in a rigid porous medium, a situation similar to that for which de Gennes developed the reptation model by analyzing the diffusion of a chain in the presence of fixed obstacles. The snakelike motion of the chain through the fixed obstacles results in a molecular weight dependence of the diffusion coefficient,[16-18] $D_\infty \sim M^{-2}$. Recent computer simulations of chain motion in a rigid random porous material[19] show even stronger molecular weight dependence. The porous glass used in our experiment provides a perfectly rigid matrix in which to examine the molecular weight dependence of diffusion. In this respect, our system stands in contrast to recent probe diffusion measurements in which the background system is itself composed of diffusing polymers sometimes at rather high concentration. We thus have a simplified situation uncomplicated by the issues of tube renewal and constraint-release that are encountered in polymer melts and entangled solutions.

Experimental Section

The four-arm and eight-arm polyisoprene stars (labeled as PI4-47 and PI8-41, respectively) used in this research were obtained from Dr. L. J. Fetters and synthesized at the University of Akron. The dispersity indices for molecular weight and arm length were specified to be less than 1.1. Linear polyisoprene and polystyrene with narrow molecular weight distributions were obtained from PolySciences, Inc., and Polymer Laboratories Ltd. The data characterizing the samples are listed in Table I.

Polystyrene samples were prepared at one-eighth of the overlap concentration, c^*, for each molecular weight. The concentration at which coils in solution start to interpenetrate[16,20] is given by $c^* = c_1/[\eta]$, where $[\eta]$ is the intrinsic viscosity of the polymer in the solvent and c_1 is a constant which depends on the coil packing model; $c_1 = 1$ was chosen for our calculations. This method was used in order to maintain a consistent reduced concentration level in all samples. Polystyrene was dissolved in 2-fluorotoluene (2FT), a thermodynamically good solvent which can be refractive index matched with the porous glasses at temperatures close to room temperature. *trans*-Decahydronaphthalene (TD) was used as the solvent for polyisoprene as dn/dc is approximately 2 times greater than in 2FT. All measurements with polyisoprene were done at four different concentrations corresponding to $c^*/6$, $c^*/5$, $c^*/4$, and $c^*/3$. The value of c^* for linear polyisoprene in TD was estimated from the measured values of the intrinsic viscosity $[\eta]$ for linear polyisoprene in toluene. In the case of the star polymers, the effect of branching on $[\eta]$ was taken into account by using the calculated values of the ratio of $[\eta]$ of stars to that of linear polymers in Θ solution.[21,22] It should be noted that the measured quantity of particular interest in this study, D_∞/D_0, is not sensitive to the absolute value of c^*. A very small quantity (approximately 0.1% by weight) of an antioxidant was added to the polyisoprene samples to prevent oxidation.

The controlled pore glasses in this study were identical with those used in the work of Bishop et al.[10,11] Three different glasses with narrow pore size distributions with pore radii (characterized by mercury intrusion porosimetry) of 703, 893, and 1866 Å (henceforth labeled as R703, R893, and R1866) with respective porosities ϕ = 0.46, 0.72, and 0.62 were used. Electron micrographs show the pore space to be a well-connected, random network of uniform pores. Adsorption of polymer on the pore walls was minimized by silanizing the porous glass fragments. Details of the silanizing procedure are described elsewhere.[23] No significant changes were found when D_∞ was repeatedly measured in a typical sample over a period of 3 months, indicating that adsorption was successfully minimized. Even if adsorption did play a small role, the relative differences between the behavior of the eight-arm, four-arm, and linear polymers are unlikely to be seriously influenced since adsorption is expected to be similar in these chemically identical species.

Experiments were performed in a typical dynamic light scattering apparatus. The scattering volume was fully contained within a single fragment of porous glass. The scattering from the stationary glass matrix served as a strong local oscillator for the production of heterodyne correlation functions. The working temperature was chosen to optimize the local oscillator strength relative to the scattering from the polymer solution in the pores. The intensity autocorrelation function, $C(q,t)$, was analyzed to obtain the diffusion coefficient of the polymer in the pore space. The wave vector, q, is related to the scattering angle by $q = 4\pi n/\lambda_0 \sin(\theta/2)$ where λ_0 is the wavelength in vacuo, n is the refractive index of the solvent, and θ is the scattering angle. The scattering angle was chosen to satisfy the conditions $qR_G < 1$ and $qR_p < 0.7$, where R_G is the polymer radius of gyration and R_p is the pore radius. The first condition $qR_G < 1$ corresponds to probing length scales larger than the radius of gyration of the molecules resulting in the measurement of the translational diffusion of the molecules without any contribution from internal modes. The second condition ensures that the length scale probed is at least equal to

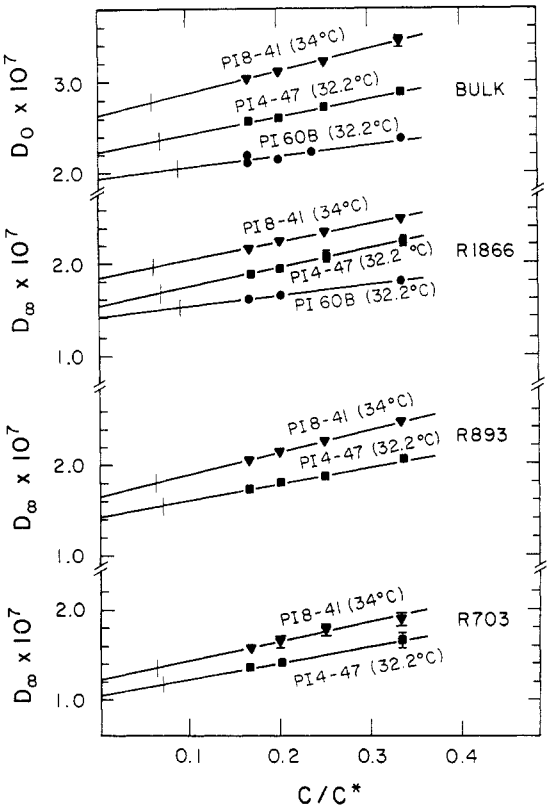

Figure 1. Concentration dependence of the diffusion coefficient in bulk (D_0) and the macroscopic diffusion inside the porous glass (D_∞). Data are shown for four-arm (PI4-47), and eight-arm (PI8-41) polyisoprene star polymers and linear polyisoprene (PI 60B) in each of the glasses: R1866, R893 and R703. The abscissa is the concentration of the solution (c) relative to the overlap concentration (c^*). For linear and star architecture polyisoprene in TD, c^* was estimated from the measured values of c^* for linear polyisoprene in toluene, as discussed in the text. The measured quantity of interest, D_∞/D_0, is quite insensitive to the absolute value of c^*. The tick marks on each curve show the concentrations at which D_∞/D_0 was extracted for subsequent analysis.

several pore radii and hence the measured diffusion coefficient can be identified as the macroscopic diffusion coefficient. Previous studies[10] have shown empirically that for values of $qR_p < 0.7$, the effective diffusion coefficient in the glass has reached its asymptotic value, D_∞.

Results and Discussion

I. Weakly Confined Star and Linear Polymers ($\lambda_H < 0.1$). The measured values of D_∞, the macroscopic diffusion coefficient in the porous glass, and D_0, the diffusion coefficient in the unbounded solution, are plotted as a function of concentration in Figure 1. [Note: In the chemical engineering literature the notation is often different than ours: the diffusion coefficient in free solution at infinite dilution is frequently denoted by D_∞, while the coefficient associated with diffusion over macroscopic distance in the porous medium is called D. Our notation emphasizes the fact that in a porous medium, the diffusion result depends on the length scale of the measurement and D_∞ is the asymptotic value at large distance scale (small q).] The values of D_∞ and D_0 were consistently extrapolated to a concentration at which the value for the diffusion, D_0, was 6% greater than its corresponding value at $c = 0$ (shown by the tick marks in Figure 1). It is important to note here that the quantity of interest, D_∞/D_0, is not very sensitive to this choice. This particular choice of concentration keeps our data comparable to those of the previous linear polystyrene studies.[11] Since the glasses used in our study are the same as those used in ref 11, we use the values of X_0 previously determined for these glasses at a concentration of $c = c^*/8$. Since X_0 could be different from that which would be obtained by extrapolation to zero concentration (but not by more than approximately 5%), we chose to extract data from our experiments at concentrations consistent with those of ref 11 rather than extrapolate to zero concentration. Unfortunately, direct measurements of the tortuosity ($1/X_0$) are not available for these rather small porous glass fragments (1–2 mm typical dimensions).

The values for D_∞, the macroscopic diffusion coefficient in the porous glass, and D_0, the diffusion coefficient of the same polymer in unbounded solution at the same temperature, are tabulated in Table II. The values of D_∞ correspond to measurements at a scattering angle of 25°, chosen to satisfy the empirical condition $qR_p < 0.7$ (discussed above). Occasional checks were made at 15° and 35° to confirm that we were in the low q asymptotic limit. The hydrodynamic radius, R_H, was calculated from measured diffusion in the unbounded solution by using the Stokes–Einstein relationship, $R_H = k_B T/(6\pi\eta_0 D_0)$ where k_B is Boltzmann's constant, T is the temperature, and η_0 is the solvent viscosity. Examining the results for the eight-arm and four-arm polymers in Table II, we find that for the same fractional reduction of D_∞/D_0 in each glass, the λ_H value for the eight-arm polymer is lower than that of the four-arm polymer. In other words, for a given confinement parameter, λ_H, the eight-arm star would have a lower diffusion coefficient than the four-arm star in each of the three glasses. Comparing the data for the star polymers with those of the linear polymers, the qualitative picture that clearly emerges is as follows. For a given λ_H

$$(D_\infty/D_0)_{\text{eight-arm}} < (D_\infty/D_0)_{\text{four-arm}} < (D_\infty/D_0)_{\text{linear}} \quad (1)$$

A combination of phenomenological theories for diffusion of point particles in random porous media and microscopic theories for diffusion of rigid spheres and flexible polymers in pores of ideal geometry has been used to interpret the data. We presume the following relation

$$D_\infty = X_0 f(\lambda_s) D_0 = X_0 D_p \quad (2)$$

where $\lambda_s = R_s/R_p$ and R_s is the radius of the sphere, X_0 is the intrinsic conductivity of the porous medium ($1/X_0$ is the tortuosity), and $f(\lambda_s)$ is the size dependent fractional reduction in the diffusion due to hydrodynamic effects alone (assuming that no other specific polymer–wall interactions exist). The D_p in eq 2 is the diffusion coefficient associated with the relaxation of concentration gradients over short length scales in the pore fluid. D_p represents the modified diffusion in the pores due to the hydrodynamic effects of the constraining pore walls whereas D_∞ is the phenomenological coefficient for transport over large distances in the porous material as a whole, including the effects of the structural features of the porous network. The structural effects of the porous medium and the hydrodynamic effects are not always strictly separable. However, for small values of λ_H and for a well-connected pore structure with a narrow pore size distribution, eq 2 is valid to first approximation as confirmed by measurements of the diffusion of linear polystyrene in such glasses.[11] In ref 11 the data on linear polystyrene were fit to

$$D_\infty/D_0 = X_0 f(\kappa\lambda_H) \quad (3)$$

where κ was chosen as a scaling factor between the hydro-

Table II
Diffusion Coefficient in Unbounded Solution (D_0), Macroscopic Diffusion Coefficient (D_∞), and Confinement Parameter (λ_H) for Different Polyisoprene Samples in Glasses R703, R893, and R1866[a]

polymer	glass	working temp, °C	$10^7 D_0$, cm²/s	$10^7 D_\infty$, cm²/s	λ_H	D_∞/D_0
PI8-41 (eight-arm)	R703	34	2.77	1.35	0.069	0.487
	R893	34	2.77	1.80	0.055	0.650
	R1866	34	2.77	1.96	0.026	0.708
PI4-47 (four-arm)	R703	32.2	2.37	1.16	0.078	0.489
	R893	32.2	2.37	1.54	0.062	0.650
	R1866	32.2	2.37	1.68	0.030	0.709
PI-60A (linear)	R893	32.2	2.01	1.40	0.073	0.697
PI-60B (linear)	R893	41.3	2.39	1.60	0.074	0.670
	R1866	32.2	2.05	1.50	0.034	0.730
PI-34 (linear)	R893	39.7	3.49	2.49	0.049	0.713

[a] D_∞ and D_0 are measured at the same temperature in each case.

Table III
Values of κ Obtained by Fitting Diffusion Data for Each Sample in Each Porous Glass to Eq 3

	κ		
polymer sample	glass R703	glass R893	glass R1866
PI8-41	0.94 ± 0.07	0.94 ± 0.09	0.88 ± 0.10
PI4-47	0.82 ± 0.07	0.83 ± 0.09	0.78 ± 0.08
PI-60A		0.40 ± 0.06	
PI-60B		0.54 ± 0.08	0.44 ± 0.07
PI-34		0.43 ± 0.05	
PS[a]		0.76	

[a] Results for linear polystyrene in 2FT from ref 11 for molecular weight ranging from 17.5×10^3 to 5.75×10^5.

dynamic radius R_H and an equivalent hard-sphere radius R_s, given by $R_s = \kappa R_H$. The results were found to be consistent with hydrodynamic theories for the diffusion of isolated hard spheres in cylindrical pores: the center-line theory[24] and the more rigorous theory of Brenner and Gaydos.[12] The center-line theory considers a sphere moving along the axis of a cylinder whereas the Brenner and Gaydos theory takes into account the dependence of the hydrodynamic parameters on off-center-line positions of the diffusing particles. The fits also yielded values for the intrinsic conductivity X_0 of the glasses R703, R893, and R1866.

Data for the star polymers presented here have been fit to eq 3, using the values of X_0 of these glasses and the analytical result obtained by Brenner and Gaydos for the function f given by

$$f_{BG}(\lambda_s) = \frac{1 + (^9/_8)\lambda_s \ln \lambda_s - 1.539\lambda_s + o(\lambda_s)}{(1-\lambda_s)^2} \quad (4)$$

where $o(\lambda_s)$ contains terms which are of higher order than those explicitly retained[12] and λ_s is small ($\lambda_s \lesssim 0.1$). The numerical result for f previously calculated by Anderson and Quinn[25] is nearly identical with the above. The role played by the scaling factor κ can be understood clearly from Figures 2 and 3. As seen in Figure 2, the dependence of $D_\infty/(D_0X_0)$ on the confinement parameter λ_H falls on a distinctly different curve for each of the three polymer architectures. The solid curves drawn through the data are the theoretical functional forms of $f_{BG}(\kappa\lambda_H)$ for $\kappa = 0.92$ for the eight-arm star, $\kappa = 0.80$ for the four-arm star, and $\kappa = 0.45$ for the linear polymer (two-arm star). If the data are replotted as a function of λ_s, using the above values of κ, the three curves collapse to a universal curve as seen in Figure 3.

From the data above, the following features can be highlighted: (a) The scaling factor κ depends on the arm number (architecture) of the polymer and increases with increasing arm number. As we would expect, the greater the number of arms, the more nearly the molecule approximates a hard sphere. (b) For a given polymer architecture, κ is independent of the confinement parameter and

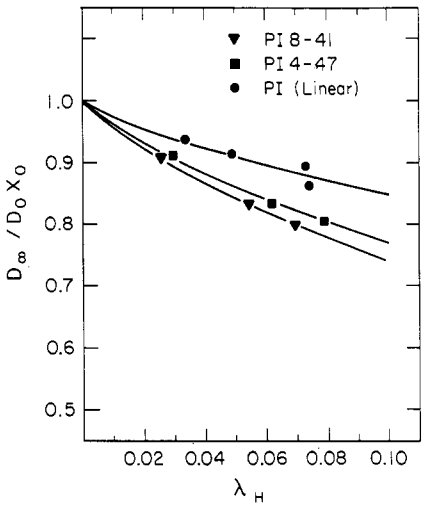

Figure 2. Effect of molecular architecture: The reduced diffusion in the pores relative to bulk, $D_\infty/(D_0X_0)$, as a function of the confinement, $\lambda_H = R_H/R_p$, for linear (PI), four-arm (PI4-47), and eight-arm (PI8-41) polyisoprene samples. The solid curves are fits to the hydrodynamic hard sphere theory of Brenner and Gaydos (eq 4 in the text) using an adjustable scaling parameter κ given by $\kappa R_H = R_s$ where R_s is the equivalent hard sphere radius. For linear, four-arm, and eight-arm samples κ = 0.45, 0.80, and 0.92, respectively.

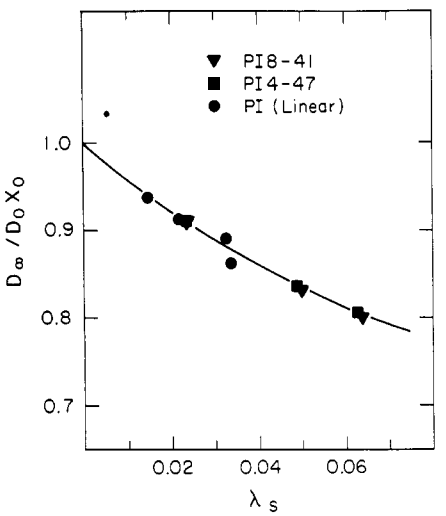

Figure 3. Reduced diffusion in the pores relative to the bulk, $D_\infty/(D_0X_0)$, for linear (PI), four-arm (PI4-47), and eight-arm (PI8-41) polyisoprene replotted as a function of $\lambda_s = R_s/R_p$ where $R_s = \kappa R_H$. Solid curve: $f_{BG}(\lambda_s)$ given by the hydrodynamic hard-sphere theory of Brenner and Gaydos (eq 4 of text).

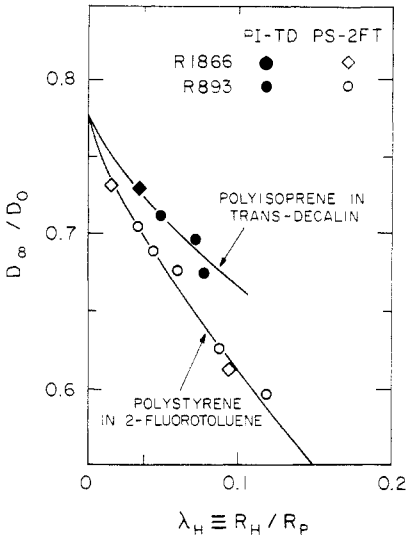

Figure 4. Comparison of the present data for linear polyisoprene with those for linear polystyrene from ref 11. Solid curves are fits to the $f_{BG}(\lambda_s)$ (eq 4 of text) where $\lambda_s = \kappa\lambda_H$ with $\kappa = 0.76$ for the polystyrene in 2-fluorotoluene and $\kappa = 0.45$ for the polyisoprene in *trans*-Decalin.

the structural factors such as the tortuosity and porosity of the glass. (c) The ratio κ depends on the polymer–solvent characteristics as seen by comparing the κ values for linear polyisoprene in TD with that for linear polystyrene in 2FT. (d) For linear polymers, κ is independent of molecular weight. Though the data for the star polymers is for a single molecular weight in each case, it is reasonable to expect κ to be independent of molecular weight.

High functionality stars are known to behave like hard spheres.[26] Our results yield $\kappa \simeq 1$ ($R_H \simeq R_s$) for the eight-arm star, indicating that for stars with arm number greater than eight the hard-sphere radius in the center-line and BG theories may be replaced by the hydrodynamic radius. It is also reasonable to expect that hindered diffusion at a given λ_H may not be dependent on arm number for molecules with a large number of arms. This, in fact, may explain some of the observations made in porous membranes.[13] In the membrane studies, star polymers with arm numbers eight, twelve, and eighteen were used and all of the branched molecules were found to behave essentially the same, irrespective of arm number, while diffusing distinctly slower than the corresponding linear molecule.

In the previous measurements on linear polystyrene[11] the scaling parameter $\kappa = 0.76$ was interpreted as possibly being due to underestimation of the pore radius by mercury intrusion porosimetry, leading to the conclusion that the hydrodynamic radius could indeed be the appropriate hard-sphere radius. In the light of our present data on star polymers, the scaling parameter κ seems to have a greater significance. The value of $\kappa \simeq 1$ that we obtain for the eight-arm polymer indicates that the estimated pore sizes by mercury intrusion porosimetry are better than expected and the κ value of 0.76 reported for polystyrene in 2FT is indeed a true conversion factor. Even if there is a small error in the pore size estimation, the differences in the scaling factor κ for the different architectures are still meaningful in a relative sense.

The data on the two linear systems, namely, PI in TD and PS in 2FT are compared in Figure 4. For a given λ_H, PI in TD is seen to have a larger diffusion coefficient in the pores relative to the unbounded solution than PS in 2FT. The data as $\lambda_H \to 0$ approach a common intercept (X_0), supporting the separability of the structural and hydrodynamic effects in these systems. The difference in the two linear systems seems then to arise from hydrodynamic effects. The data fit to the Brenner and Gaydos hydrodynamic hard-sphere theory with $\kappa = 0.76$ for PS in 2FT and $\kappa = 0.45$ for PI in TD. Considering that the solvents used in each case are good solvents for the polymer, the flexibility of the polymers may be playing a significant role. Judging by the parameters that characterize the overall effect of short range interactions,[27] the flexibility of polyisoprene is significantly greater than that of polystyrene.

To see if the radius of gyration R_G would be a better length scale, the results of the calculation of the dimensionless parameter $\rho = \langle R_H^{-1}\rangle_z R_G$ for regular star polymers[21] were used to calculate an equivalent scaling factor κ_G defined by $R_s = \kappa_G R_G$. The results for κ_G are in Table IV. It is seen that characterizing the confinement by R_G does *not* produce a universal scaling factor κ_G independent of arm number. Values of R_G/R_H from the experimental data of Roovers et al.[26] are different from the theoretical values listed in Table IV. The conclusion that R_G is not a better length scale than R_H would still not change if the Roovers et al. values of R_G/R_H are used instead. The above discussion ignores possible changes in conformation of the polymers inside the pores, and the factor κ may in fact carry information about these changes.

Table IV
Values of ρ, κ_G, and κ_H for Linear and Star Polymers[a]

no. of arms	$\rho = \langle R_H^{-1}\rangle_z R_G$[b]	$\kappa_G = R_s/R_G$[c]	$\kappa_H = R_s/R_H$
2	1.5	0.30	0.45
4	1.33	0.60	0.80
8	1.22	0.75	0.92

[a] κ_G as well as κ_H varies with molecular architecture, indicating that neither radius of gyration or hydrodynamic radius uniquely characterizes diffusion within the pores. [b] From ref 21. [c] κ_G calculated from our results for κ_H using $\kappa_G = \kappa_H/\rho$.

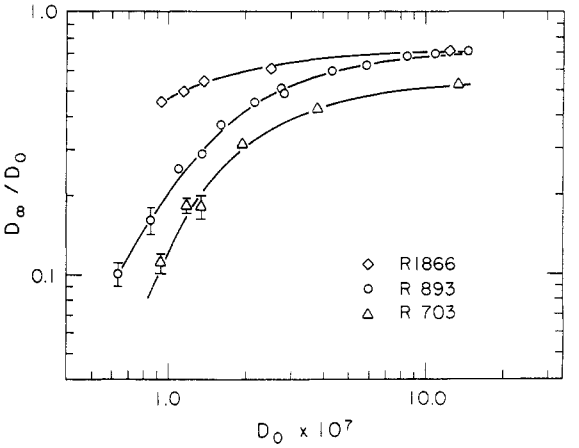

Figure 5. A double logarithmic plot of D_∞/D_0 vs D_0 for linear polystyrene in all three porous glasses. For the range of molecular weight 17.5×10^3 to 4.4×10^6 covered by these data, a clear power law dependence is not seen. Data for molecular weight below 2.05×10^6 are from ref 11.

II. Strongly Confined Linear Chains. Measurements of the macroscopic diffusion in the pores of strongly confined linear polymers have been done with the PS–2FT system. Results for the diffusion of linear polystyrene in 2FT in each of the three glasses are shown in Figure 5 as a double logarithmic plot of D_∞/D_0 vs D_0. The highest molecular weight used was $M_p = 4.4 \times 10^6$. Each sample was prepared at one-eighth of the corre-

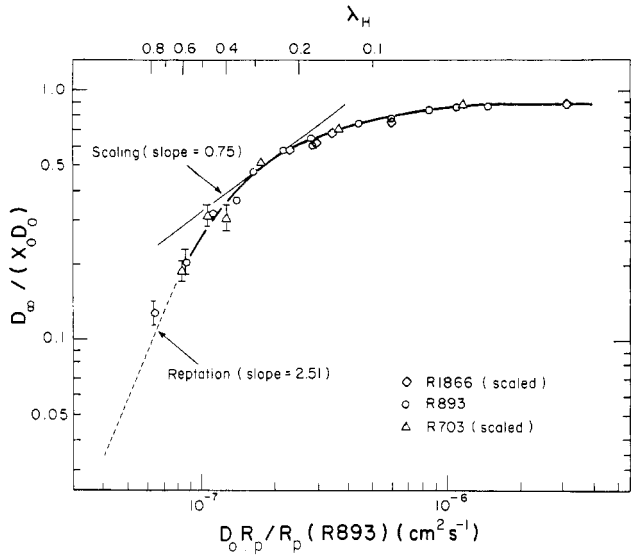

Figure 6. Scaled version of the data in Figure 5: The ordinate is scaled by the value of X_0 for each glass, and the abscissa is scaled by the ratio of the pore radius of R893 to that of each glass, as discussed in the text. Solid straight line: predicted slope from scaling theory. Dashed straight line: predicted slope from reptation theory. The values of the confinement parameter, λ_H, are shown on the upper scale.

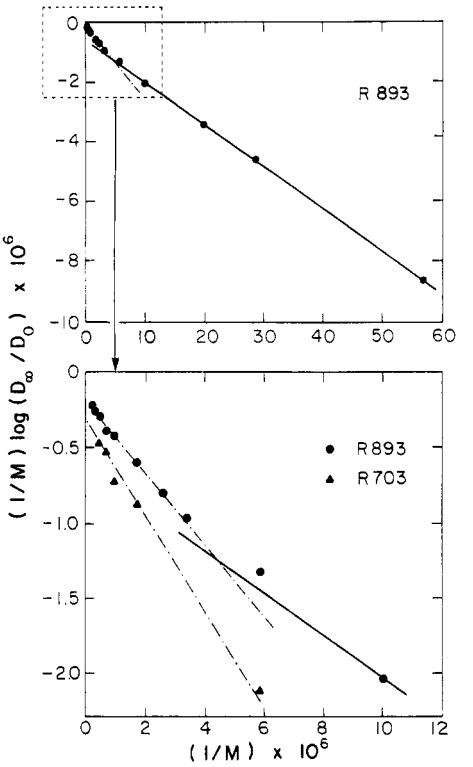

Figure 7. Plot of $(1/M)$ log (D_∞/D_0) vs $(1/M)$ for linear polystyrene–2FT in porous glasses R893 and R703. The lower panel shows data near the origin in greater detail. Solid lines represent the linear regime at weak confinement and dashed lines, the linear regime at strong confinement.

sponding overlap concentration. The general features of the three curves appear staggered along the D_0 axis, since a particular value of D_0 corresponds to a different confinement, R_H/R_p in each of the three glasses. If the abscissa of each data point in Figure 5 is multiplied by R_p/R_p (893), the ratio of the pore radius of the glass in which the measurement was made to 893 Å (the pore radius of glass R893), a rescaled universal plot is obtained as shown in Figure 6. Each abscissa corresponds to a given value of the confinement parameter λ_H, as shown on the upper scale.

The lines representing $D_\infty \sim M^{-1}$ as predicted by scaling theories and $D_\infty \sim M^{-2}$ as predicted by reptation are shown in Figure 6 for comparison with the data. Since $D_0 \sim M^{-0.57}$ for polystyrene in 2-fluorotoluene,[23] $D_\infty \sim M^{-1}$ and $D_\infty \sim M^{-2}$ correspond to slopes of 0.75 and 2.51, respectively, in the double logarithmic plot of $D_\infty/(D_0X_0)$ vs D_0R_p/R_p (893). Clearly for the range of confinements covered by the data, there is no range of molecular weights, over which a power law behavior is seen. The increasing size of the error bars at higher molecular weight is due to the weak scattered signal from the polymers inside the fragment resulting from the low concentration of the polymers in the pore volume. Further, the time scale of the relaxations becomes large, and this combined with weak signal makes the data very sensitive to external disturbances.

The possible presence of more than one length scale in the porous material could play an important role in the diffusion mechanism at strong confinements. Muthukumar and Baumgartner[41] have considered diffusion within a rigid confining matrix consisting of larger cavities of a single size interconnected by smaller passages of a single size. They predict that the effect of entropic barriers introduced by the additional length scale would dominate polymer diffusion. Their theoretical model predicts two linear regimes, corresponding to the weak and strong confinement limits, in a plot of $(1/M)$ log (D_∞/D_0) vs $1/M$. Figure 7 is such a plot of our data at higher confinement along with previous data from ref 11. The two linear regimes are clearly suggested in the plot of the extensive data in glass R893, while the data in glass R703 apparently span only the linear regime corresponding to strong confinement. Thus, the model of entropic barriers seems to be appropriate in describing diffusion at these confinements.

At the higher molecular weights, the scattered light intensity correlation function shows a faster relaxation mode in addition to that due to translational diffusion. This could be evidence of longitudinal internal modes in the confined chain. Even though the scattering angle is chosen to satisfy $qR_G < 1$ where R_G is the radius of gyration in unbounded solution, for higher confinements the chains may be significantly deformed making the contributions from the internal modes more significant. Correlation functions in these cases were analyzed by an inverse Laplace transform, using Provencher's CONTIN program,[28,29] to reveal two decay modes; the relaxation rate of the slower mode was associated with macroscopic diffusion.

Probing higher confinements than those reported here by the QELS technique may still be possible by using glasses of smaller pore size together with lower molecular weight polymers. However, problems of weak signal resulting from low concentration within the pores would still exist.

Conclusions

Comparative measurements were made of the diffusion of star and linear polymers in rigid media containing random, well-connected pores with narrow pore size distributions. For a given confinement, λ_H, defined as the ratio of the hydrodynamic radius of the polymer to the pore radius, molecular architecture is found to affect the hindered diffusion. At a given λ_H, star polymers diffuse more slowly than linear polymers, with the eight-arm star polymer diffusing more slowly than the four-

arm star polymer. A scaling parameter, κ, has been calculated that relates the hydrodynamic radius to an equivalent hard-sphere radius. For a given polymer–solvent system, the value of κ is independent of the parameters characterizing the porous glass and is found to depend only on the molecular architecture. The effective radius of a linear polymer is found to be smaller than the bulk solution value R_H. As the number of arms increases, the effective radius approaches the bulk solution value. There is also an indication that the polymer–solvent combination affects the value of κ, as seen by the differences between the polyisoprene–TD and polystyrene–2FT systems.

In summary, the length scale characterizing the hydrodynamic effects of constraining walls on polymer diffusion is not the hydrodynamic radius derived from diffusion in dilute unbounded solution. The equivalent hard-sphere radius depends on molecular architecture and possibly the stiffness of the polymer chain. It is not clear how the polymer–solvent interaction affects the hindered diffusion.

De Gennes[16] has discussed the effect of pore walls on intramolecular hydrodynamics of chains and predicts a smaller effective R_H than the bulk solution value. Our results are in agreement with this prediction. Sedimentation velocity and intrinsic viscosity measurements by Roovers et al.[26] has indicated that highly branched polymers behave hydrodynamically almost like hard spheres in dilute solution, in agreement with our results of $\kappa \simeq 1$ for the eight-arm star polymer. Comparison of the hindered diffusion of model branched polymers with that of linear molecules has been done in melts[30–32] where the measurements agree with the predictions of the reptation model. The situation in the semidilute and entangled solutions is more complicated by additional contributing mechanisms such as constraint release or tube renewal[33–35] and the "noodle effect".[36] NMR[37,38] and dynamic light scattering measurements[39] have been done in these concentration regimes.

For dilute solutions far below the overlap concentration, the recent membrane transport measurements with polyisoprene[13] (the same polymer used in our measurements) report the same qualitative trend seen in our results; i.e., linear molecules diffuse faster than the branched structures for the same R_H/R_p ratio. However the membrane study indicates that the characteristic size controlling pore diffusion is approximately 35% smaller than R_H for the linear chains whereas it is approximately 20% larger than R_H for all the branched structures. Our data indicate that the characteristic size controlling pore diffusion is approximately 55% smaller than R_H for the linear chains and becomes almost equal to R_H for the eight-arm polymer. The interpretation of our measurements is simpler due to the fact that the knowledge of the partitioning coefficient is not necessary. However, the membrane study covers a wider range of confinements than reported here. Considerable differences are noted between results from various membrane studies[1,3,4] using different polymer–solvent systems. This, along with the marked differences that we saw between the polystyrene and polyisoprene, further supports the possibility that over and above the molecular architecture, other parameters of the polymer and the polymer–solvent system also affect the effective characteristic size controlling porous diffusion. Early results from size-exclusion chromatography[40] showed no differences between the elution times of linear and branched structures. More recent[14,15] studies, however, indicate that star polymers elute from chromatography columns as if their hydrodynamic radii were larger than the measured ones by a small amount (5–10%).

In the case of strongly confined linear chains, up to the highest molecular weight and confinement probed by these data, no clear power law dependence of D_∞ on molecular weight was found. The continuously falling curve in Figure 6 with no power law dependence agrees qualitatively with the predictions of the computer simulations,[19] though the porous medium used here is uniform as compared to the truly random porous structure developed in the simulations. Our data also indicate that the presence of an additional length scale in the porous network could play an important role in the diffusion of strongly confined chains. For investigating higher confinements, the QELS technique does not appear to be promising.

Acknowledgment. Our thanks to Professors R. Guyer and M. Muthukumar for many useful discussions. We would also like to thank Dr. M. Bishop of Dow Chemical for discussions of his extensive work on linear polystyrene samples in the same porous glasses used in our work. Dr. W. Haller of the National Bureau of Standards provided one of the porous glass samples, and the star polymers were a gift from Dr. L. J. Fetters of Exxon Research Laboratories. Support for this work by the U.S. Air Force Office of Scientific Research under Contract No. AFOSR 87-001 is gratefully acknowledged.

References and Notes

(1) Cannell, D. S.; Rondelez, F. *Macromolecules* **1980**, *13*, 1599.
(2) Guillot, G.; Léger, L.; Rondelez, F. *Macromolecules* **1985**, *18*, 2531.
(3) Deen, W. M.; Bohrer, M. P.; Epstein, N. B. *AIChE J.* **1981**, *27*, 952.
(4) Bohrer, M. P.; Patterson, G. D.; Carroll, P. J. *Macromolecules* **1984**, *17*, 1170.
(5) Colton, C. K.; Satterfield, C. N.; Lai, C.-J. *AIChE J.* **1975**, *21*, 289.
(6) Tennikov, M. B.; Belen'kii, B. G.; Nesterov, V. V.; Anan'eva, T. D. *Colloid J. USSR (Engl. Transl.)* **1979**, *41*, 526.
(7) Klein, J.; Grüneberg, M. *Macromolecules* **1981**, *14*, 1411.
(8) Dozier, W. D.; Drake, J. M.; Klafter, J. *Phys. Rev. Lett.* **1986**, *56*, 197.
(9) Karger, J.; Lenzher, J.; Pfeifer, H.; Schwabe, H.; Heyer, W.; Panowski, F.; Walf, F.; Zdanov, S. P. *J. Am. Ceram. Soc.* **1983**, *66*, 69.
(10) Bishop, M. T.; Langley, K. H.; Karasz, F. E. *Phys. Rev. Lett.* **1986**, *57*, 1741.
(11) Bishop, M. T.; Langley, K. H.; Karasz, F. E. *Macromolecules* **1989**, *22*, 1220.
(12) Brenner, H.; Gaydos, L. J. *J. Colloid Interface Sci.* **1977**, *58*, 312.
(13) Bohrer, M. P.; Fetters, L. J.; Grizzuti, N.; Pearson, D. S.; Tirrel, M. V. *Macromolecules* **1987**, *20*, 1827.
(14) Hadjichristidis, N.; Guyot, A.; Fetters, L. J. *Macromolecules* **1978**, *11*, 668.
(15) Roovers, J.; Toporowski, P. M. *Macromolecules* **1981**, *14*, 1174.
(16) de Gennes, P.-G. *Scaling Concepts in Polymer Physics*; Cornell University Press: Ithaca, NY, 1979.
(17) de Gennes, P.-G. *J. Chem. Phys.* **1971**, *55*, 572; **1980**, *72*, 4756.
(18) Doi, M.; Edwards, S. F. *J. Chem. Soc., Faraday Trans 2* **1978**, *74*, 1789, 1802, 1818; **1979**, *75*, 38.
(19) Baumgartner, A.; Muthukumar, M. *J. Chem. Phy.* **1987**, *5*, 3082.
(20) Nystrom, B.; Roots, J. *Prog. Polym. Sci.* **1982**, *8*, 333.
(21) Burchard, W. *Adv. Polym. Sci.* **1983**, *48*, 1.
(22) Yamakawa, H. *Modern Theory of Polymer Solutions*; Harper and Row: New York, 1971.
(23) Bishop, M. T. Ph.D. Thesis, University of Massachusetts, Amherst, MA, 1987.
(24) Happel, J.; Brenner, H. *Low Reynolds Number Hydrodynamics*; Prentice-Hall: Englewood Cliffs, NJ, 1965.
(25) Anderson, J. L.; Quinn, J. A. *Biophys. J.* **1974**, *14*, 130.
(26) Roovers, J.; Hadjichristidis, N.; Fetters, L. J. *Macromolecules* **1983**, *16*, 214.
(27) Brandup, J.; Immergut, E. H. *Polymer Handbook*; Wiley-Interscience: New York, 1975.

(28) Provencher, S. W. *Makromol. Chem.* **1979**, *180*, 201.
(29) Provencher, S. W.; Hendrix, J.; de Maeyer, L.; Paulsson, N. J. *Chem. Phys.* **1978**, *69*, 4273.
(30) Klein, J.; Fletcher, D.; Fetters, L. J. *Nature (London)* **1983**, *304*, 526.
(31) Bartels, C. R.; Crist, B., Jr.; Fetters, L. J.; Graessley, W. W. *Macromolecules* **1986**, *19*, 785.
(32) Antonietti, M.; Sillescu, H. *Macromolecules* **1986**, *19*, 798.
(33) Daoud, M.; de Gennes, P.-G. *J. Polym. Sci., Polym. Phys. Ed.* **1979**, *17*, 1971.
(34) Klein, J. *Macromolecules* **1981**, *14*, 460.
(35) Graessley, W. W. *Adv. Polym. Sci.* **1982**, *47*, 67.
(36) Fujita, H.; Einaga, Y. *Polym. J. (Tokyo)* **1985**, *17*, 1131.
(37) von Meerwall, E.; Tomich, D. H.; Hadjichristidis, N.; Fetters, L. J. *Macromolecules* **1982**, *15*, 1157.
(38) von Meerwall, E.; Tomich, D. H.; Grigsby, J.; Pennisi, R. W.; Fetters, L. J.; Hadjichristidis, N. *Macromolecules* **1983**, *16*, 1715.
(39) Lodge, T. P.; Wheeler, L. M. *Macromolecules* **1986**, *19*, 2983.
(40) Grubisic, Z.; Rempp, P.; Benoit, H. *J. Polym. Sci., Polym. Lett. Ed.* **1975**, *5*, 753.
(41) Muthukumar, M.; Baumgartner, A. *Macromolecules* **1989**, *22*, 1937, 1941.

Registry No. Polyisoprene, 9003-31-0; polystyrene, 9003-53-6.

Effect of Water on Diblock Copolymers in Oil: Large Aggregates, Micelles, and Microemulsions

Kathleen A. Cogan and Alice P. Gast*

Department of Chemical Engineering, Stanford University, Stanford, California 94305.
Received April 20, 1989; Revised Manuscript Received July 5, 1989

ABSTRACT: We present a dynamic light scattering study of polystyrene–poly(ethylene oxide) diblock copolymers in cyclopentane, a selective solvent for polystyrene. We find that a trace amount of water has a profound effect on the structures formed in dilute solution due to the compatibility of poly(ethylene oxide) and water. We investigate changes in hydrodynamic radius as a function of copolymer and water concentration for two diblock copolymers of varying composition and molecular weight. Unusually large stable aggregates form in solutions with low water content. Addition of water promotes monodisperse spherical micelles in solutions of large aggregates as well as in solutions containing only single chains. Further addition of water results in a solution of swollen micelles, i.e., a polymeric microemulsion. At very low copolymer concentrations, saturated micelles exhibit a sharp increase in hydrodynamic size.

Introduction

Block copolymers in a selective solvent can form structures due to their amphiphilic nature. Above the critical micelle concentration (cmc), the free energy of the system is lower if the block copolymers associate into micelles rather than remain dispersed as single chains. Often the micelles are spherical, with a compact core of insoluble blocks surrounded by a corona of soluble blocks.[1-3] Addition of a second solvent, compatible with the insoluble block and immiscible with the continuous phase, leads to the formation of swollen micelles or a polymeric microemulsion.

In this paper, we describe the effects of changing water and copolymer concentrations for polystyrene–poly(ethylene oxide) (PS–PEO) diblock copolymers in cyclopentane at 23 °C. Since water is a solvent for poly(ethylene oxide) and cyclopentane is a near Θ solvent for polystyrene (T_Θ = 19.5 °C)[4], the micelles consist of a poly(ethylene oxide) core swollen with water and protected by a polystyrene corona. Previous morpholigical studies of polymeric microemulsions have involved graft and block copolymers in ternary solvent mixtures containing toluene, water, and either an alcohol or an amine acting as a cosurfactant.[5-9] Although the cosurfactant increases the dispersion capability of the copolymers, it adds to the complexity of the system since it is generally soluble in both the continuous and dispersed phases. We investigate the dispersion of water in cyclopentane, a highly immiscible system, by PS–PEO block copolymers alone. Others[10] have prepared oil-in-water microemulsions from block copolymers without cosurfactants.

Trace amounts of water are inevitably found in most organic solvents. Water strongly affects the structures formed by PS–PEO block copolymers beyond inducing microemulsions. We find unusually large structures in our driest solutions that disappear upon the addition of small amounts of water. Others[11-13] have observed large aggregates in solutions of PS–PEO diblock copolymers in selective solvents for polystyrene and have attributed their existence to the crystallizability of poly(ethylene oxide). We also believe the crystallizability of PEO is responsible for the large aggregates we find in dry cyclopentane; at higher water concentrations, water molecules dissolve the PEO chains reducing the driving force for formation of large aggregates.

Unusual structures have also been observed in ionic surfactant solutions with very low water content. Small rigid aggregates form in solutions of AOT (sodium 1,4-bis(2-ethylhexyl)sulfobutanedioate) in isooctane with water contents on the order of 25 ppm.[14] The heads of the surfactants are linked together by hydrogen bonds, with water acting as a "gluing" agent.[15,16] Unlike micelles at equilibrium, the aggregate size does not change as the temperature is varied from 0 to 50 °C. These structures are similar to large PEO–PS aggregates in that strong interactions between hydrophilic moieties promote the formation of structures not present at higher water contents.

0024-9297/90/2223-0745$02.50/0